Inorganica Chimica Acta 421 (2014) 500–506

Contents lists available at ScienceDirect

Inorganica Chimica Acta

journal homepage: www.elsevier.com/locate/ica

Metal-dependent dimensionality in divalent metal coordination polymers containing diphenate and bis(4-pyridylformyl)piperazine ligands

Lucas E. Weingartz [b], Curtis Y. Wang [a], Robert L. LaDuca [b,*]

[a] Diamond Bar High School, Diamond Bar, CA 91765, USA
[b] Lyman Briggs College and Department of Chemistry, Michigan State University, East Lansing, MI 48825, USA

ARTICLE INFO

Article history:
Received 16 May 2014
Received in revised form 2 July 2014
Accepted 9 July 2014
Available online 22 July 2014

Keywords:
Copper
Cobalt
Coordination polymer
Diphenate
Ferromagnetism

ABSTRACT

Hydrothermal synthesis has afforded a pair of paramagnetic divalent metal diphenate coordination polymers containing long-spanning bis(4-pyridylformyl)piperazine (4-bpfp) ligands. Single-crystal X-ray diffraction revealed an important structure directing role on the part of the metal coordination environment. [Cu(diphenate)(4-bpfp)]$_n$ (**1**, diphenate = biphenyl-2,2′-dicarboxylate) shows a system of 2-fold parallel interpenetrated (4,4) grid coordination polymer layers. {[Co(diphenate)(4-bpfp)]·2H$_2$O}$_n$ (**2**) possesses *anti-syn* bridged {Co(OCO)$_2$}$_n$ infinite 1-D chains, linked into a non-interpenetrated 6^6 3-D diamondoid net. A variable temperature magnetic susceptibility study of **2** indicates the presence of weak ferromagnetic coupling, concomitant with single-ion effects. Thermal properties of these materials are also discussed.

1. Introduction

Vigorous interest continues towards the synthesis and structural elucidation of metal-organic coordination polymer crystalline solids. These materials have potent utility in several useful applications [1,2], such as gas storage [3], small molecule separation [4], ion exchange [5], heterogeneous catalysis of organic transformations [6], explosives detection [7] and second harmonic generation [8]. Myriad aesthetic structural topologies can be seen in these solid phases, predicated on variance in metal coordination and the donor disposition within anionic or formally neutral organic components [9]. Subtle variations in organic components can impart very significant differences in physical properties [10].

The diphenate ligand (biphenyl-2,2′-dicarboxylate, Scheme 1) has been an efficacious choice for the design and construction of coordination polymers, in the presence or absence of dipyridyl-type tethering coligands [11–16]. The conformationally flexible σ bond between the aromatic rings of diphenate allows it to adopt various twisted and locked conformations, resulting in varied topologies depending on the supramolecular environments provided by different metal coordination preferences. For example, [Cu(diphenate)(4,4′-bpy)]$_n$ (4,4′-bpy = 4,4′-bipyridine) manifests square planar coordination at copper and a twisted diphenate conformation. This results in [Cu(diphenate)]$_n$ helices linked by 4,4′-bpy into a 3-D network with a relatively uncommon 4-connected **cds** $6^5$8 topology [11]. Altering the coordination environment to a distorted tetrahedral geometry by moving to divalent zinc afforded [Zn(diphenate)(4,4′-bpy)]$_n$ [12]. This material possessed similar linked helical metal-diphenate chains and 4-connected metal atom nodes as seen in its copper congener. However, its overall topology was significant altered, showing the unique example of a uninodal $4^2 8^4$ 2-fold interpenetrated 3-D network.

Our group has successfully employed the long-spanning, hydrogen-bonding capable dipyridyl/piperazine neutral tethering ligands bis(4-pyridylmethyl)piperazine (4-bpmp) and its amide derivative bis(4-pyridylformyl)piperazine (4-bpfp) (Scheme 1) in the preparation of topologically novel divalent metal carboxylate coordination polymers [17–23]. By way of example, {[Zn$_3$(H$_2$O)$_4$(tca)$_2$(4-bpmp)$_2$]·8H$_2$O}$_n$ (tca = tricarballylate) displayed a unique 3,4-connected 3-D interpenetrated net with a simple $(6^3)(6^5 8)$ topology [17]. [Co$_3$(oba)$_3$(4-bpmp)$_2$]$_n$ (oba = oxybis(benzoate) manifested a striking trimer-based 8-connected self-penetrated network with $4^4 5^{17} 6^7$ topology [18]. {[Cd$_4$(bdc)$_4$(4-bpfp)$_3$(H$_2$O)$_2$]·8H$_2$O}$_n$ (bdc = 1,4-benzenedicarboxylate) exhibited a complex trinodal self-penetrated 3-D network, while [Zn$_2$Cl$_2$(bdc)(4-bpfp)$_2$]$_n$ showed the first known example of threaded-loop 1D + 1D → 1D parallel chain interpenetration [19]. In this contribution we report the synthesis and structural characterization of a pair of paramagnetic divalent

* Corresponding author. Mailing address: Lyman Briggs College, E-30 Holmes Hall, Michigan State University, East Lansing, MI 48825 USA.
E-mail address: laduca@msu.edu (R.L. LaDuca).

http://dx.doi.org/10.1016/j.ica.2014.07.026
0020-1693/

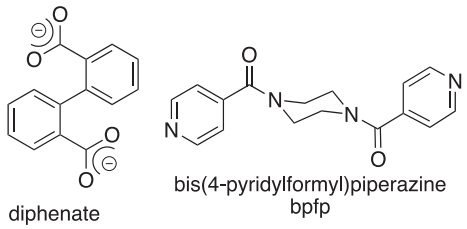

Scheme 1. Ligands used in this study.

metal diphenate coordination polymers containing 4-bpfp, $[Cu(diphenate)(4\text{-bpfp})]_n$ (**1**) and $\{[Co(diphenate)(4\text{-bpfp})]\cdot 2H_2O\}_n$ (**2**). Thermal properties of **1** and **2** were investigated, along with the variable temperature magnetic susceptibility behavior of **2** due to its carboxylate bridged paramagnetic metal ions.

2. Experimental

2.1. General considerations

Metal salts and diphenic acid were obtained commercially. Bis(4-pyridylformyl)piperazine (4-bpfp) [24] was prepared via a published procedure. Water was deionized above 3 MΩ-cm in-house. Elemental Analysis was carried out using a Perkin Elmer 2400 Series II CHNS/O Analyzer. IR spectra were recorded on powdered samples on a Perkin Elmer Spectrum One instrument. Thermogravimetric analysis was performed on a TA Instruments Q50 thermal analyzer under flowing N_2. Variable temperature magnetic susceptibility data for **2** (2–300 K) were collected on a Quantum Design MPMS SQUID magnetometer at an applied field of 0.1 T. After each temperature change the sample was kept at the new temperature for 5 min before magnetization measurement to ensure thermal equilibrium. The susceptibility data was corrected for diamagnetism using Pascal's constants, and for the diamagnetism of the sample holder.

2.2. Preparation of $[Cu(diphenate)(4\text{-bpfp})]_n$ (1)

$Cu(NO_3)_2\cdot 2.5H_2O$ (69 mg, 0.30 mmol), 4-bpfp (110 mg, 0.37 mmol), diphenic acid (90 mg, 0.37 mmol), and 1 mL of 1.0 M NaOH were placed into 10 mL distilled H_2O in a Teflon-lined acid digestion bomb. The bomb was sealed and heated in an oven at 100 °C for 24 h, whereupon it was cooled slowly to 25 °C. Blue blocks of **1** (96 mg, 53% yield based on Cu) were isolated after washing with distilled water and acetone, and drying in air. *Anal.* Calc. for $C_{30}H_{24}CuN_4O_6$ **1**: C, 60.05; H, 4.03; N, 9.34. Found: C, 59.64; H, 4.06; N, 9.21%. IR (cm^{-1}): 3056 (w), 2983 (w), 2886 (w), 1623 (s), 1612 (s), 1592 (s), 1543 (m), 1504 (w), 1460 (w), 1439 (s), 1423 (s), 1351 (s), 1293 (m), 1280 (m), 1253 (w), 1233 (s), 1182 (w), 1169 (w), 1151 (m), 1104 (w), 1088 (w), 1073 (w), 1054 (m), 1048 (w), 1025 (w), 1014 (s), 979 (w), 950 (w), 909 (m), 890 (w), 877 (w), 836 (s), 809 (w), 778 (m), 766 (s), 746 (s), 737 (s), 711 (s), 685 (s), 659 (m).

2.3. Preparation of $\{[Co(diphenate)(4\text{-bpfp})]\cdot 2H_2O\}_n$ (2)

$CoSO_4\cdot 7H_2O$ (104 mg, 0.37 mmol), 4-bpfp (110 mg, 0.37 mmol) and diphenic acid (90 mg, 0.37 mmol) and 1 mL of 1.0 M NaOH were placed into 10 mL distilled H_2O in a Teflon-lined acid digestion bomb. The bomb was sealed and heated in an oven at 120 °C for 48 h, whereupon it was cooled slowly to 25 °C. Orange blocks of **2** (87 mg, 37% yield based on Co) were isolated after washing with distilled water and acetone, and drying in air. *Anal.* Calc. for $C_{30}H_{28}CoN_4O_8$ (with loss of one molar equivalent of water on long-term storage) **2**: C, 58.73; H, 4.27; N, 9.61. Found: C, 58.11 H, 3.99; N, 9.36%. IR (cm^{-1}): 3553 (w), 1621 (s), 1607 (s), 1575 (s), 1557 (s), 1546 (s), 1500 (m), 1468 (s), 1435 (s), 1397 (s), 1370 (w), 1329 (w), 1289 (s), 1265 (s), 1218 (w), 1155 (m), 1122 (w), 1103 (w), 1059 (m), 1050 (w), 1006 (s), 971 (w), 942 (w), 907 (m), 877 (w), 835 (s), 810 (w), 762 (w), 749 (s), 733 (s), 716 (s), 675 (s), 657 (m).

3. X-ray crystallography

Single-crystal diffraction data for **1** and **2** were collected using a Bruker-AXS Apex2 CCD instrument. Reflection data was acquired using graphite–monochromated Mo Kα radiation (λ = 0.71073 Å). The reflection data were integrated with SAINT [25]. Lorentz and polarization effect and empirical absorption corrections were applied with SADABS [26]. The structures were solved using direct methods and refined on F^2 using SHELTXL [27]. All non-hydrogen atoms were refined with anisotropic thermal parameters. Hydrogen atoms bound to carbon atoms were placed in calculated positions and refined with isotropic thermal parameters using a riding model. Pertinent crystallographic data for **1** and **2** are listed in Table 1.

4. Results and discussion

4.1. Synthesis and spectral characterization

Hydrothermal reaction of a metal salt, diphenic acid, and 4-bpfp generated crystalline samples of **1** and **2**. The infrared spectra of both were consistent with the organic components seen in their crystal structures. Features corresponding to pyridyl or phenyl ring flexing and puckering modes were observed in the region between 600 and 820 cm^{-1}. Medium intensity bands in the range of ~1600 to ~1200 cm^{-1} arise from stretching modes of the aromatic rings of the dicarboxylate ligands and pyridyl rings within the dicarboxylate and dipyridyl ligands. Asymmetric and symmetric C–O

Table 1
Crystal and structure refinement data for **1** and **2**.

Compound	**1**	**2**
Empirical Formula	$C_{30}H_{24}CuN_4O_6$	$C_{30}H_{28}CoN_4O_8$
Formula weight	600.07	631.50
Crystal system	orthorhombic	monoclinic
Space group	*Pbca*	*C*2/*c*
a (Å)	15.0393(15)	31.550(2)
b (Å)	17.0865(17)	9.3123(6)
c (Å)	19.2422(19)	9.4941(6)
β (°)	90	97.7650(10)
V (Å^3)	4944.6(9)	2763.9(3)
Z	8	4
D_{calc} (g cm^{-3})	1.612	1.513
μ(mm^{-1})	0.941	0.682
Minimum/maximum transmission	0.901	0.947
hkl Ranges	$-18 \leqslant h \leqslant 18$, $-20 \leqslant k \leqslant 20$, $-23 \leqslant l \leqslant 23$	$-37 \leqslant h \leqslant 35$, $-11 \leqslant k \leqslant 10$, $-11 \leqslant l \leqslant 11$
Total reflections	38 545	8283
Unique reflections	4536	2497
R_{int}	0.0840	0.0427
Parameters	370	195
R_1 (all data)[a]	0.0761	0.0690
R_1 ($I > 2\sigma(I)$)[a]	0.0416	0.0643
wR_2 (all data)[b]	0.1171	0.1870
wR_2 ($I > 2\sigma(I)$)[b]	0.0984	0.1803
Max/min residual (e^-/Å^3)	0.523/−0.547	0.712/−0.512
G.O.F.	1.003	1.074

[a] $R_1 = \Sigma||F_o| - |F_c||/\Sigma|F_o|$.
[b] $wR_2 = \{\Sigma\,[w(F_o^2 - F_c^2)^2]/\Sigma\,[wF_o^2]^2\}^{1/2}$.